Katholieke Universiteit Leuven

Departement Elektrotechniek

ESAT-SISTA/TR 2005-168

An open source short echo time MR quantitation software solution: AQSES [1]

Arjan W. Simonetti[2] Jean-Baptiste Poullet[2]
Diana M. Sima[2] Bart De Neuter[2] Leentje Vanhamme[2]
Philippe Lemmerling [2] Sabine Van Huffel[2]

January 2006
Submitted to the *NMR in Biomedicine*.

[1]This report is available by anonymous ftp from *ftp.esat.kuleuven.ac.be* in the directory *pub/sista/dsima/reports/SISTA5-168.pdf*

[2]ESAT-SCD-SISTA, K.U. Leuven, Kasteelpark Arenberg 10, B-3001 Leuven-Heverlee, Belgium, Tel. 32/16/32 43 11, Fax 32/16/32 19 70, E-mail: *sabine.vanhuffel@esat.kuleuven.be*. This work was supported by **Research Council KUL:** GOA-AMBioRICS, several PhD/postdoc & fellow grants; **Flemish Government: FWO:** PhD/postdoc grants, projects, G.0407.02 (support vector machines), G.0269.02 (magnetic resonance spectroscopic imaging), G.0270.02 (nonlinear Lp approximation), G.0360.05 (EEG, Epileptic), research communities (ICCoS, ANMMM); **IWT:** PhD Grants; **Belgian Federal Science Policy Office:** IUAP P5/22 ('Dynamical Systems and Control: Computation, Identification and Modelling'); **EU:** BIOPATTERN, ETUMOUR.

Abstract

This paper describes AQSES, a software package for quantitation of short echo time magnetic resonance spectra. AQSES contains a graphical user interface and is available online from www.esat.kuleuven.ac.be/sista/members/biomed/new/ under an open source license, which means that the source code is freely available and easy to adapt to specific needs of the user. The quantitation problem is mathematically formulated as a separable nonlinear least squares fitting problem, which can be solved numerically using a variable projection procedure. A macromolecular baseline is incorporated into the fit via nonparametric modeling, efficiently implemented using penalized splines. The graphical user interface is optimized to perform quantitation in batch mode and is therefore very suitable for spectroscopic imaging data. Numerous preprocessing methods like phase-, frequency- and eddy current correction are implemented. Unwanted components such as residual water can be removed with a maximum-phase FIR filter or the HLSVD-PRO filter. AQSES has been tested on simulated MR spectra with several types of nuisance and on short echo time *in vivo* proton MR spectra. Results show that AQSES is robust, easy to use and very flexible due to its open source license.

An open source short echo time MR quantitation software solution: AQSES

Arjan W. Simonetti Jean-Baptiste Poullet Diana M. Sima
Bart De Neuter Leentje Vanhamme Philippe Lemmerling
Sabine Van Huffel

ESAT-SISTA, K.U. Leuven

Kasteelpark Arenberg 10, B-3001 Leuven-Heverlee, Belgium

corresponding author:

Prof. Dr. Ir. Sabine Van Huffel

Tel. 016/32 17 03, Fax. 016/32 19 70

Email: Sabine.VanHuffel@esat.kuleuven.be

Web: http://www.esat.kuleuven.be/sista/members/vanhuffel.html

January 12, 2006

Abstract

This paper describes AQSES, a software package for quantitation of short echo time magnetic resonance spectra. AQSES contains a graphical user interface and is available online from `www.esat.kuleuven.ac.be/sista/members/biomed/new/` under an open source license, which means that the source code is freely available and easy to adapt to specific needs of the user. The quantitation problem is mathematically formulated as a separable nonlinear least squares fitting problem, which can be solved numerically using a variable projection procedure. A macromolecular baseline is incorporated into the fit via nonparametric modeling, efficiently implemented using penalized splines. The graphical user interface is optimized to perform quantitation in batch mode and is therefore very suitable for spectroscopic imaging data. Numerous preprocessing methods like phase-, frequency- and eddy current correction are implemented. Unwanted components such as residual water can be removed with a maximum-phase FIR filter or the HLSVD-PRO filter. AQSES has been tested on simulated MR spectra with several types of nuisance and on short echo time *in vivo* proton MR spectra. Results show that AQSES is robust, easy to use and very flexible due to its open source license.

Keywords: quantitation, MR spectroscopy, short echo time, metabolites

Abbreviations:

AQSES: Accurate Quantitation of Short Echo time domain Signals

FIR: Finite Impulse Response

HLSVD-PRO: Hankel-Lanczos Singular Value Decomposition with partial reorthogonalization

PM: Performance Measure

Lip1: Lipids at 1.3 ppm

Lip2: Lipids at 0.9 ppm

1 Introduction

Accurate quantitation of metabolites from short echo time *in vivo* magnetic resonance spectroscopy (MRS), such as proton spectra from the human brain, may be a very important aid in the correct noninvasive diagnosis of pathology. The development of easy-to-use quantitation software is a challenging task, and very important for the acceptance of spectroscopy in the clinic. For example, magnetic resonance spectroscopic imaging can be of help in brain tumour diagnosis [1], but only if accurate quantitation of the metabolites of interest can be performed [2]. Ultimately, the (multivariate) analysis of quantified (spectroscopic imaging) data can lead to the construction of classification images, which can be a direct aid in the diagnosis of the patient's illness [3, 4].

Analysis of *in vivo* short echo time proton spectra is complicated by broad baseline signal contributions, resonance line-shape distortions and the complexity of the spectra due to overlap. In spite of these difficulties it is very interesting to quantitate short echo time spectra if compared with long echo time spectra. The quantified values are a better reflection of the true concentration of the metabolites, since short echo time spectra are less affected by transverse relaxation. Furthermore, J-coupling modulations are minimized, signal-to-noise ratio (SNR) is optimized and short echo time acquisitions can be used to detect additional metabolites including glutamate, glutamine and myo-inositol. Several studies show that the level of myo-inositol may aid tumor classification and grading [5, 6, 7] and total glutamate/glutamine levels have been found to be significantly different between low grade oligodendrogliomas and astrocytomas [8]. In addition, the baseline may be an important feature, since lipid signals may be relevant in the differentiation of metastases from high-grade gliomas [9] or as indicator of grade [10, 11].

Each metabolite has a typical time response in a proton NMR experiment, depending on the number of chemically different protons attached to the compound. This time response has, in theory, the shape of a sum of complex damped exponentials. During an *in vivo* experiment, the time-domain signal will consist of responses from all metabolites (including macromolecules), noise and suppressed water. Spectra of metabolites that are visible during *in vivo* spectroscopy can also be measured *in vitro*, and these signals

can be grouped in a database of metabolite profiles. To perform accurate quantitative analysis of an *in vivo* time-domain signal, it can be modeled as a linear combination of a selection of the profiles in the database plus a *baseline* signal that accounts for the presence of macromolecules. The quantities of interest, the metabolite *concentrations*, can be estimated from the weighting coefficients (amplitudes) of the linearly combined *in vitro* profiles. The linear combination should allow for small corrections in spectral parameters like frequency shifts, damping corrections and phase shifts, as well, since these parameters may vary from measurement to measurement [12].

The baseline is a smooth, broadband, low amplitude signal, that gives an underlying trend to the *in vivo* signal, when visualized in the frequency-domain. Its shape can vary and it is in general unpredictable, especially in pathological cases. For this reason, a good choice is found in identifying it as a smooth curve using nonparametric modeling [13].

Important contributions in the field of fitting short echo time NMR signals include [13] and [14, 12]. Some of the differences and similarities between the optimization technique implemented in AQSES (Accurate Quantitation of Short Echo time-domain Signals) and the procedure used in LCModel [13] are:

- AQSES fits the complex time-domain signal, which is the data acquisition domain; LCModel fits the real part of the frequency-domain signal;
- AQSES uses a FIR filtering technique to remove undesired resonances from specific frequency ranges;
- In both methods, the baseline is non-parametrically modeled using penalized splines in the frequency-domain; the fact that AQSES fits in the time-domain is not a problem, because a smoothing criterion that involves an inverse Fourier transformed spline basis can be used;
- The AQSES method comes with an advanced JAVA based – platform independent – user interface, which allows usage in scientific as well as clinical environments.

Comparing AQSES to the recent contribution in [14, 12] (QUEST), we highlight the following differences:

- A nonparametric baseline is recovered in QUEST using heuristic methods, where several steps are involved: truncation, partial fitting, subtraction, and final fitting. Its performance is sensitive to the choice of the number of truncated data points and the model order for the baseline fit. The algorithm in AQSES uses only one common optimization problem for the fitting of both the model and the baseline. It is thus less prone to accumulated errors.

- In reference [14], an augmented Fisher information matrix (inspired by [15]) is used, but it is not clear how to choose the value for the number of effective parameters involved in the computation of confidence bounds. In this respect, the discussion in [16], based on asymptotic nonlinear regression theory, clarifies the way the confidence bounds can be automatically estimated for the procedure in AQSES.

A major difference of AQSES compared to LCModel as well as QUEST is that the source code of AQSES is available under the Lesser GPL, an OSI approved open source license. This license forces that changes made to the framework of AQSES by other parties are distributed under the same license. It also allows users to create their own plug-ins and distribute them under a different license, even as closed source. Plug-ins do not have to be in a specific language, but can be included in the language they were originally programmed in. This can potentially lead to a very fast improvement of the software, when plug-ins for other file formats or specific preprocessing modules are added by third parties.

2 Theory and methods

2.1 The AQSES framework

To increase the usability, AQSES has been embedded in an application framework which controls the optimization method [17]. In general, an application framework provides a set of abstract classes and interfaces, called hot spots that can be combined to create an application. For AQSES, the framework provides hot spots for plug-ins to read or write, to preprocess, to quantitate, to export and to visualize MRS and MRSI data. The software is developed in Java and is platform independent (*e.g.*, Windows, Linux, OSX and Solaris). The graphical user interface (GUI) of the framework is written using the Swing library. The GUI is intended to run in two different modes. The *clinical mode* hides most of the complexity by using templates, while the *research mode* provides the user with all features. The AQSES GUI is template driven, which means that scripts can be built that contain the settings for preprocessing and quantitation. Templates can be saved and used to easily redo experiments or to start processing in batch mode. At the moment the AQSES GUI accepts MRS and MRSI data coming from Philips (SDAT/SPAR format) and SIEMENS (RDA format), or data stored in a Matlab (The MathWorks, inc., Version 4) or text file. It is easy to add plug-ins to read or write other formats by implementing some of the hot spots. After loading, the data can be visualized in the time- or frequency-domain and is presented to the user in a 3D graph. It is also possible to work with multiple data sets at the same time, which are stored in a project. The preprocessing methods included at the moment are eddy current correction (Klose [18]), HLSVD-PRO [19], zero filling and (manual) phase and frequency correction. There are two quantitation methods available in the AQSES GUI at the moment, AQSES and HLSVD-PRO. Both methods have been compiled for Windows and Linux and have been made accessible to the Java code, to make sure that the software can run on both platforms. The data and the results of the quantitation methods are visualized in a separate window and can be exported to a text file or a Matlab file.

AQSES and the HLSVD-PRO algorithm are implemented in FORTRAN 77. The main

optimization part of AQSES is carried out using an extension of the Levenberg-Marquardt algorithm, which accepts linear bounds constraints, in the DN2GB implementation written by David M. Gay [20]. FORTRAN is used since well-tested and optimized numerical libraries (*e.g.*, LAPACK, Blas) exist.

2.2 Mathematical formulation

For the quantitation of short echo time NMR signals, we consider that we are given a "metabolite database", which is a set $\{v_k, \text{ for } k = 1, \ldots, K\}$ of complex-valued time series of length m, representing *in vitro* measured NMR responses. An *in vivo* measured NMR signal y, which is another complex-valued time series of length m, will satisfy the model

$$y(t) = \widehat{y}(t) + \varepsilon_t := \sum_{k=1}^{K} \alpha_k \left(\zeta_k\right)^t v_k(t) + b(t) + w(t) + \varepsilon_t, \quad t = t_0, \ldots, t_{m-1}, \tag{1}$$

where $\alpha_k, \zeta_k \in \mathbb{C}$ are unknown parameters that account for amplitudes of the metabolites in the database and for the necessary corrections of the database signals, due to inherent differences between the acquisition techniques. In fact, the complex amplitudes α_k and the complex signal poles ζ_k can be written as (with $j = \sqrt{-1}$):

$$\alpha_k = a_k \exp(j\phi_k), \qquad \zeta_k = \exp(-d_k + jf_k), \tag{2}$$

where a_k are the real amplitudes, ϕ_k are the phase shifts, d_k are damping corrections, and f_k are frequency shifts.

In (1), $b(t)$ represents the chemical part that is not modeled. It represents the response of the unknown components that are not included in the database. We will refer to this part of the signal as being the "baseline", which contains a large number of macromolecular broad components. In mathematical terms, b is characterized by the assumption that its Fourier transformation is a smooth function. The term $w(t)$ refers to the residual water component (as well as other possible nuisance terms), whose frequency positions are relatively known. This term can sometimes be included in the database, but in other

cases it is *filtered out* using a filter like FIR [21] or HLSVD-PRO; however, the region(s) that should be filtered out of the *in vivo* signal should be specified by the user. Finally, the ε_t term denotes an unknown noise perturbation with zero mean.

The identification of complex amplitudes α_k, and complex poles ζ_k, for $k = 1, \ldots, K$, can be accomplished by minimizing the least squares criterion: $\sum_{t=t_0,\ldots,t_{m-1}} |y(t) - \widehat{y}(t)|^2$.

For the nonparametric modeling of the baseline, we construct a basis of splines [22, 23] and put the discretized splines as columns in a matrix A. An arbitrary nonlinear function can be approximated as a linear combination of spline functions. The coefficients in this linear combination are unknowns that must be identified. We denote these linear coefficients by $c_1, \ldots, c_n$ (or by $\mathbf{c} \in \mathbb{C}^n$, when stacked in a column vector). Thus, the discretization of a nonlinear function approximated with splines (in our case, the Fourier transform of the baseline b) can be written in matrix notation as the matrix-vector product $A \cdot \mathbf{c}$.

A regularization operator D is defined to measure the smoothness of the baseline in the frequency-domain. We can take D as the discrete second-order differential operator $\begin{bmatrix} -1 & 2 & -1 & & 0 \\ & \ddots & \ddots & \ddots & \\ 0 & & -1 & 2 & -1 \end{bmatrix}$, first-order differential operator $\begin{bmatrix} -1 & 1 & & 0 \\ & \ddots & \ddots & \\ 0 & & -1 & 1 \end{bmatrix}$, zero-order differential operator $\begin{bmatrix} 1 & & 0 \\ & \ddots & \\ 0 & & 1 \end{bmatrix}$, or some combination.

Since the goal is to reconstruct a smooth baseline in the frequency-domain, while still fitting in the time-domain, we use back-transformation of the basis matrix A to the time-domain, with the discrete inverse Fourier transform. In order to fit the model and the smooth baseline at the same time, we consider the regularized nonlinear least squares criterion

$$\min \frac{1}{m} \sum_{t=t_0}^{t_{m-1}} |y(t) - \widehat{y}(t)|^2 + \lambda^2 \|D\mathbf{c}\|^2, \tag{3}$$

where in $\widehat{y}$ we incorporate the sum of metabolites (as in (1)), and the baseline $b = \mathcal{A} \cdot \mathbf{c}$ as the inverse Fourier transformation of the frequency-domain baseline $A \cdot \mathbf{c}$. We ignore for the moment the nuisance term w. For the case when w is included, a more general formulation, which fits *filtered* signals to *filtered* models will be discussed in subsection 2.2.2. In (3), λ is a fixed *regularization (penalty) parameter*, and the whole term $\lambda^2 \|D\mathbf{c}\|^2$ is responsible

for ensuring a certain degree of smoothness to the baseline b. The value that we give to λ controls the degree of smoothness; this value can be automatically selected using a generalized cross validation criterion (see [16] for more details).

Cramer-Rao bounds, specially adapted for semiparametric nonlinear regression [16], can also be computed as a by-product of the quantitation procedure. They correspond to all the spectral parameters for the metabolites of interest (linear and nonlinear parameters, as well) and give an indication about the uncertainty of the final quantified parameters. If the given bounds are small enough relative to the corresponding parameter value, then it means that the computed value is reliable. If a large bound is found for a certain component, then the computed parameters might be unreliable. This is not due to a faulty minimization process; instead, it is due to poor signal-to-noise ratio, or incomplete database of metabolites.

2.2.1 Algorithmic details

When the baseline term and the water term are ignored, the nonlinear least squares problem becomes

$$\min \frac{1}{m} \sum_{t=t_0}^{t_{m-1}} \left| y(t) - \sum_{k=1}^{K} \alpha_k \left(\zeta_k\right)^t v_k(t) \right|^2 = \min_{\boldsymbol{\alpha},\boldsymbol{\zeta}} \frac{1}{m} \left\| \mathbf{y} - \Phi(\boldsymbol{\zeta})\boldsymbol{\alpha} \right\|_2^2, \tag{4}$$

where $\mathbf{y}$ is a column vector containing $y(t_0), \ldots, y(t_{m-1})$, $\boldsymbol{\alpha}$ and $\boldsymbol{\zeta}$ are defined as K-dimensional column vectors from the respective variables, and the $m \times K$ matrix $\Phi(\boldsymbol{\zeta})$ has elements of the form:

$$\Phi_{ik} = (\zeta_k)^{t_i} v_k(t_i) = \exp\left((-d_k + jf_k)t_i\right) \cdot v_k(t_i), \tag{5}$$

Problem (4) is a *separable* problem, where linear parameters $\boldsymbol{\alpha}$ can be projected out of the least squares problem, and only a smaller sized nonlinear least squares problem remains to be solved for the nonlinear variables $\boldsymbol{\zeta}$, via an iterative minimization algorithm of the Levenberg-Marquardt type [24]. This technique is called *variable projection* (VARPRO

[25, 26]). One of its advantages is that it does not encounter numerical problems when some amplitudes α_k are nearly zero. When a baseline is also fitted, the variable projection optimization is augmented such that the penalty on the baseline's smoothness is also incorporated. In this case, the VARPRO method is much more efficient than optimizing the nonlinear least squares problem (3) directly, over all linear and nonlinear parameters without separation, since there are many more linear parameters (in $\boldsymbol{\alpha}$ and $\mathbf{c}$) than nonlinear ones ($\boldsymbol{\zeta}$).

As initial values for the nonlinear parameters we set zeros, which means that we start the optimization with no spectral corrections to the signals in the database. It is possible to impose *prior knowledge* in the form of linear bounds on the nonlinear parameters, or linear equalities between some variables of the same sort among d_k or f_k.

2.2.2 Using a filter

A filter can be used to remove irrelevant information from the *in vivo* NMR signal. For instance, a pass-band FIR filter can be used to select only the frequency region of interest. The FIR filter in AQSES originates from the implementation of [21]; it is a maximum-phase FIR filter that is automatically optimized in order to remove the water component from an *in vivo* NMR signal.

Applying a FIR filter to a vector (a discrete signal) involves a convolution operation. This is however a simple and fast computation. When such an operation is applied to the measured signal, it must also be taken into account by the fitting model. In other words, a filtered measured signal will be fitted with a filtered model plus a filtered baseline.

The design of the filter is performed outside the actual fitting method of AQSES. Such a filter consists of a vector of coefficients; the length of the filter and the coefficients are optimized during the automatic filter design. Let $h_1, \ldots, h_p$ denote the filter coefficients. Then a discrete-time signal v, *i.e.*, a vector of length m, can be convolved with the filter giving the filtered signal u (of length $m - p + 1$), according to

$$u_i = \sum_{l=1}^{p} h_l v_{i+l-1}, \qquad i = 1, \ldots, m - p + 1.$$

A FIR filter is a linear operator that commutes with the sum; however, it does not commute with the *modified* sum of metabolites, since the shifts and corrections on the spectral parameters involve nonlinear operations. Thus, we cannot just filter the signals in the database and apply the same procedure as for unfiltered signals; instead, the filter should be used explicitly during the iterative minimization in AQSES. The changes that are involved in the filtered version of the minimization are the following three:

- the *in vivo* signal $\mathbf{y}$ is replaced throughout with its filtered version;
- the matrix Φ constructed from the metabolite profiles as in (5) will be replaced at each function (and Jacobian) evaluation with a matrix whose columns are filtered versions of the columns of the original Φ;
- the spline matrix $\mathcal{A}$ is replaced throughout with its filtered version (each column is thus separately filtered).

2.3 Simulated examples and *in vivo* quantitation

The *in vitro* metabolite profiles in this paper have been acquired on a 1.5 T Philips NT Gyroscan using a PRESS sequence with an echo time of 23 ms, and a PRESS box of $2 \times 2 \times 2\,\mathrm{cm}^3$. To each sample, two reference compounds were added, situated at 0.0 ppm and at 8.44 ppm. All raw FIDs were Eddy current corrected using Klose's method in the AQSES GUI, and the spectra were frequency shifted such that the second reference peak was at 8.44 ppm. All profiles were normalized with respect to the 8.44 ppm resonance in the sample of creatine, to ensure that absolute comparison between metabolites is possible. Metabolite profiles of lipids at 1.3 ppm and 0.9 ppm have been artificially created from the creatine resonance. At these resonances, macromolecular lipids are known to be present in pathologies, but have to be simulated since no pure profiles of these compounds can be measured *in vitro*. Therefore, absolute values of these metabolites cannot be compared with the other metabolites. Their simulation was performed by removing the creatine signal from the spectrum with HLSVD-PRO, followed by addition of a single resonance at 1.3 or 0.9 ppm. Finally, all metabolite profiles have been processed by HLSVD-PRO (from

4.4 ppm to 7.0 ppm) to remove the residual water resonance and some artifacts within that region. As example, the N-acetylaspartate (NAA) profile is plotted in Figure 1.

Five experiments have been designed to test the robustness and the accuracy of AQSES. The **first** one emphasizes on the accuracy level that can be reached for the parameter estimation. A large amount of simulated signals were created for that purpose. Each simulated signal consisted of a linear combination of 8 metabolite profiles in the basis set, *i.e.*, myo-inositol (Myo), creatine (Cr), phosphorylcholine (PCh), glutamate (Glu), NAA, lactate (lac), lipid at 1.3 ppm (Lip1), and lipid at 0.9 ppm (Lip2). These metabolites were chosen since they have been found to be important in the detection of many pathologies. Note that no nuisance components such as baseline, noise or water, were added to the simulated signals. The parameters for amplitude, damping, phase and frequency for each simulated signal were chosen in the following way: first, meaningful parameters were estimated from a set of 98 short echo time *in vivo* MRSI spectra acquired from normal brain tissue. Estimations were obtained using AQSES in a controlled way in which results were visually inspected and outliers removed. This was done to mimic a real world situation and to obtain sensible mean values and standard deviations (SD) for all parameters. Then, for the simulated signals, the amplitudes were restricted to the mean ±3*SD (only positive), the damping was restricted to the mean ±10 Hz. The phases were set variable between -45 and 45 degrees, but were the same for all profiles in one simulated signal. The frequencies were restricted to their zero ±4.5 Hz. This resulted in a set of data (set 1) with 200 simulated spectra.

For each metabolite k in the simulated signal l, the true amplitudes ($a_{k,l}$) were compared to the estimated ones ($\tilde{a}_{k,l}$) obtained with AQSES by means of a performance measure (PM) defined as:

$$PM_k = 100\sqrt{\frac{\sum_{l=1}^{200}(a_{k,l} - \tilde{a}_{k,l})^2}{\sum_{l=1}^{200} a_{k,l}^2}}, \tag{6}$$

A low PM reflects a high performance, and is a percentage measure of the difference between estimated and true amplitudes.

The **second** experiment extends the results of the first one for larger databases, *i.e.*, with more metabolite profiles. We took the same simulated spectra (set 1) as in the first experiment, but three more metabolite profiles were added to the basis set: taurine (Tau), alanine (Ala) and glucose (Glc). We chose these metabolites because they are known to be important metabolites that do not have strong correlation with the metabolites that were already inside the basis set.

The **third** experiment shows the influence of water, baseline and noise on the estimated amplitudes. We considered the same basis set as in the first experiment (using 8 metabolite profiles in AQSES). Five sets of simulated signals were constructed:

set 2 = set 1 with water resonance nuisance at 4.7 ppm,

set 3 = set 1 with low white noise (SNR = 25),

set 4 = set 1 with high noise (SNR = 7),

set 5 = set 1 with baseline distortion

set 6 = set 1 with water, baseline and high noise.

The baseline distortion was based on information from Table 1 in [27]; the baseline is the sum of gaussians referred to as lip3, lip4, lip5, mm2, mm3 and mm4 in that paper. The water profile has been extracted from an *in vivo* spectrum by means of HLSVD-PRO. The noise is a circular[1] gaussian white noise with a standard deviation σ defined as the ratio of the reference peak height at 8.44 ppm and the SNR, both in the frequency-domain. To determine the influence of water, baseline and noise, the PM has been studied. As illustration, we plotted a simulated spectrum from set 4 and from set 6 in Figure 2.

In the **fourth** experiment, AQSES was validated using an *in vitro* sample. This test solution contained 9 metabolites of known concentrations: Cr, NAA, Glu, Gln, Myo, PCh, Glycerophosphorylcholine (GPCh), Tau and Lac. The basis set used in AQSES was: Cr, NAA, Glu, Myo, PCh, Tau and Lac. Glu was selected to fit the combination of Glu and

[1] equal variances for real and imaginary part

Gln, since Glu and Gln have similar profiles and are highly correlated. The combination of PCh and GPCh was fitted with PCh since these metabolites have equivalent profiles, and are therefore not distinguishable. The true and estimated proportions of metabolites have been compared, the proportion of metabolite k being the ratio of the concentration of metabolite k and the total concentration (all metabolites).

In the **last** experiment, *in vivo* NMR signals from a database containing MRSI spectra from normal tissue (122 spectra selected from data of four volunteers), gliomas of grade II (GII, 90 spectra selected from data of six patients) and Glioblastoma multiforma (GBM, 59 spectra selected from data of five patients) were processed. The goal of this part is to show that AQSES provides sensible results in accordance to the literature. For the specific acquisition procedure and settings, see [3]. The basis set was identical to the one in the first experiment. We also display metabolic images obtained from a patient with a GBM (I-1285 from the INTERPRET database [28]) that underwent spectroscopic imaging. The metabolic images have been obtained by processing all spectra of the patient in batch mode by AQSES, using the same basis set as before.

3 Results

3.1 The AQSES interface

The two most important windows of the AQSES interface are the main and results window. The main window (Figure 3) allows the user to configure AQSES. The menus and buttons in box A provide easy access to all kinds of functionalities of the software. This includes load, open and save operations, manual phasing, eddy current correction, frequency correction, access to the HLSVD-PRO water removal, and the AQSES fitting algorithm. It is also possible to load a template, in order to automatically execute a series of processing modules. The list on the right (box B) shows the number of spectra in the currently running project. It is possible to process one, or a selection of the spectra at a time. We can also visualize one or more spectra in box C in time or frequency-domain. In Figure 3, two spectra from the database containing MRS signals from volunteers are depicted. This gives an indication of the noise in the *in vivo* spectra, and, thus, of the problem complexity. Below the spectra, the AQSES settings are displayed (box D). On the left, the tabs provide information about baseline settings, the specific database used to fit the spectra and the region to be filtered out by the FIR filter. On the right, the user can select profiles from the database and plot them on the spectra, for visualization purposes.

The results window (Figure 4) shows the fitted amplitudes, dampings, frequencies, phases and their Cramer-Rao bounds on the left. Using the top buttons, the results can be saved to a Matlab file or plain text for further processing. The residual, baseline, individual components and fit of the spectrum are displayed in order to visually evaluate the results. Since the spectra are filtered with a FIR filter that slightly alters the phase of the signal in the region of interest, spectra may look distorted compared to the original. However, this has no effect on the results of quantitation, since all profiles in the basis set have been filtered with the same settings (see 2.2.2 and [21]).

3.2 Robustness of AQSES

Figure 5 shows a boxplot of the distribution of the amplitudes found by AQSES for the *in vivo* spectra that were used to estimate meaningful values for the simulated signals. Values for the amplitudes are in agreement with expected values based on visual inspection of the spectra.

The result of the **first** experiment is shown in the first row of Table 1. The PM is fluctuating from 0.19 for NAA to 6.09 for lactate. A closer inspection of the difference between the estimated and simulated values (Figure 6, left) shows that in most cases the fit is almost perfect. In some cases the fitting fails. It is also clear that often Lac is misfitted, leading to its large PM. The overall performance decreases when more nuisance components are added, as can be seen in the right part of Figure 6, where the difference between the estimated and simulated values for data set 6 are plotted. In contrast to the situation where no nuisance components are present, all spectra contribute now evenly to the PM.

The **second** simulated example shows the results when the number of metabolites in the basis set and in the simulated spectra are not the same (second row of Table 1). The PM is of the same order of magnitude as in the first experiment, except for Myo and PCh. Typically Tau, Ala and Glc were 1 to 2 orders of magnitudes smaller than the rest of the Metabolites (not shown). Note that Myo and PCh have peaks in the same frequency range as Tau and Glc. However, the errors were close to 0 in 80% of the cases. This shows that AQSES is not very sensitive to the choice of the basis set if its components are not strongly correlated.

The **third** experiment investigates the robustness of AQSES against the additional nuisance components such as noise, baseline and water resonances. The PM are reported in Table 1 for each simulation set.

The extreme values are mainly present in the overlapping peaks, *i.e.*, Lac and Lip1. The maximum-phase filter removes satisfactorily the water component, if we inspect the differences between the PM in set 1 and set 2 in Table 1 (rows 1 and 3). Indeed, the

water resonance does not significantly affect the relative square error (p-values of the one-sided t-tests > 0.05 for each metabolite). The PM for different noise levels confirms the stability of AQSES against noise. At low noise values, the PM does not increase dramatically for all metabolites, except for Lac and Lip1. At high noise, the PM of Lip1 keeps increasing strongly, while the PM of Lac is more stable. The PMs of the 5 main metabolite profiles show stability against noise (columns 1 to 5 in Table 1). The baseline affects each component, but mainly Myo, PCh and Glu. Myo and Glu are wider and therefore are more likely to be fitted by the baseline. The concentration of PCh being smaller than other components, it can be more sensitive to the addition of a baseline. Cr is less affected by the baseline. We notice that the PM of NAA and Cr remain under 11% in all cases. The largest PM value is kept under 35%.

For the **fourth** experiment, the true and estimated proportions of the amplitudes of the metabolites in the test sample are reported in Figure 7. The errors between the true and the estimated proportions are relatively small (all $< 26\%$) and especially for the metabolites in higher concentration ($< 8\%$). Note that the summation of estimated Glu and Gln gives a good estimation ($\approx 6\%$) of the true sum while the individual estimations of Glu and Gln are not as good ($\approx 25\%$, data not shown). This is due to the high degree of correlation between these two metabolite profiles.

For the **last** experiment, we show in Figure 8 the averaged estimated amplitudes obtained with AQSES, for 8 metabolites of the three classes normal, grade II and GBM. NAA and Cr decrease with the grade of the tumor. A large difference occurs between the concentration of NAA in normal and glioma tissues. Myo, PCh and Glu exhibit much less variations. We note a small increase in Glu and PCh with the grade of glioma. Ordered from the highest to the lowest in concentration for comparable metabolites (*i.e.*, without Lip1 and Lip2, see 2.3), we have for normal brain: NAA, Glu, Cr, Myo, Lac and PCh; for GII: Glu, Lac, Cr, NAA, Myo and PCh; and for GBM: Lac, Glu, PCh, Cr, NAA and Myo. We note that Lac, Lip1 and Lip2 strongly increase with the grade of the tumor.

The AQSES GUI also allows the user to display metabolic images as in Figure 9. In

this example, the affected region is clearly visible on the T2 weighted image (Figure 9a). The tumor region can also be identified from almost all metabolic images (see Figure 9 (d, f, g, h, and i)). The concentrations of NAA and Cr are lower in the tumor region, while the concentrations of Lac, Lip1 and Lip2 are larger in that region. Myo decreases in the tumor, but this contrast is less apparent than in the case of NAA or Cr. Very interesting to see is the increase of PCh, Lac and Lip2 in the indicated regions. This region exhibits a small increase in intensity on the T2-weighted image as well. Also noticeable is the low Glu concentration in the region of the ventricle.

4 Discussion

The AQSES framework provides an easy-to-use environment for quantitation of short echo time proton MRS spectra. It is flexible and invites users to participate in its development since it is open source and plug-in based. The implementation of methods to load, preprocess, save and export data is relatively straightforward and contributed plug-ins by third parties will be made available for the community. The user interface provides the possibility to treat single spectra and spectra in batch mode. Procedures can be performed through templates, which facilitates an accurate and identical processing of multiple experiments throughout time.

The semiparametric model used in AQSES provides an effective way of dealing with the removal of the macromolecular baseline. In parallel, AQSES relies on the use of a frequency selective FIR filter, able to remove the residual water component and to keep the region of interest with minimal distortions. These essential features improve the estimation of concentrations for the metabolites of interest.

The VARPRO implementation of AQSES, using a modified Levenberg-Marquardt minimization algorithm, is important for fast convergence and reliable numerical computations and is less affected by local minima, since no starting values are needed for the linear parameters (including the parameters of the baseline). The nonlinear parameters (*e.g.*, frequency shifts or damping corrections) are initialized with zeros, which is the most reasonable choice in the context of short echo time quantitation.

To evaluate the quality of AQSES in terms of accuracy, robustness and reliability, the results of the five experiments explained in the methods section are discussed. The first two experiments show that AQSES generates most of the time an almost perfect fit on simulated data created with stringent variations (covering a range normally found in *in vivo* situations for amplitude, damping, frequency and phase). We observed that around 90% of the fits were perfect if eight profiles were used in the database. This value decreased to 80% if Tau, Ala and Glc were additionally used. The effect of an occasional misfit is clearly visible in Figure 6. The left plot shows that only a small number of simulated spectra are erroneously fitted. However, the small number of misfitted spectra show relatively large

errors on some profiles (mostly Lac). Lac and Lip resonate at almost the same frequency. In misfitted cases, the amplitudes of the two profiles are most of the time not summed with the same phase, but with opposite phases. This leads to an overestimation of Lac. In the right plot of Figure 6, the errors are more homogeneously distributed over the spectra and profiles, which is to be expected since nuisance components for water, baseline and high noise were added to the signals.

The classical VARPRO method leaves the linear part of the model completely free such that no constraints can be imposed on the amplitude and phase. But, in theory, the phases of the metabolites are equal. Such prior knowledge should be included in the model and has been implemented in a new beta version of AQSES [29].

It has to be noted that in most cases the incorrect fit is identified by high Cramer-Rao bounds for the Lac profile. It is around 100 times higher compared to the bounds for the other profiles if the fit is incorrect.

Another important aspect is the choice of the basis set in AQSES. Indeed, overlapping metabolites can ruin the parameter estimation. When no water, noise or baseline were added, the amplitude estimation of the metabolites which were not actually in the signal (*i.e.*, Tau, Ala and Glc), were often close to zero (see experiment 2). Although these results indicate an added value of the VARPRO method over other methods, we should be careful before claiming that choosing the largest database will give the best results. A larger database will increase the complexity of the algorithm, and therefore the risk of convergence to a local minimum. Furthermore, the parameter variances will also increase, limiting the accuracy of the algorithm. Note that also a too small database is prone to error, since the metabolites included in the model would try to fit the metabolites actually contained in the signal.

Next, we investigated the nuisance parameters and their effect on the parameter estimation. Satisfactory results were obtained in the presence of a residual water component and low noise. The errors of experiment 3, sets 2 and 3 do not increase dramatically. The FIR filtering removes the water component, reducing the effects of this nuisance compo-

nent. The algorithm is robust against noise since the least squares problem that is solved is restricted to a linear combination of corrected metabolite profiles present in the signal; using metabolite profiles instead of individual peaks implies an increased robustness against noise, because correlations between spectral regions that are relatively far apart are taken into account.

At higher noise, the error on all metabolites increases, which is to be expected.

The baseline remains a crucial issue during fitting due to its large correlation with the other metabolites. Ratiney *et al.* [14] noted that the background amplitude was correlated with all metabolite amplitudes except that of Cr. Our result shows that (compared to the results of data set 1) the errors for all metabolites increase. We observe that the error on Cr increases less than the other errors. This seems to be in agreement with the observation of Ratiney *et al.* [14]. If data set 1 is combined with water, baseline and high noise nuisance, then the errors for Cr and NAA remain below 10%. Both Cr and NAA are abundant in normal brain and have isolated resonances. The errors of Glu, Lac and Lip1 approach 30%. Glu is difficult to fit since it has a high correlation with the baseline. The Lac and Lip1 are often interfering, and therefore have high errors.

The fourth experiment shows that AQSES provides good estimations for the metabolites in an *in vitro* situation. For *in vivo* data we find that the amplitudes of healthy tissue as plotted in Figure 5 are realistic and that only a minor number of outliers occur (+ signs in boxplots). Also, the *in vivo* MRS spectra of gliomas of grade II and GBM agree with the literature. As can be seen in Figure 8, the estimated amplitude of NAA decreases with the malignancy of the tumor (see, *e.g.*, [30]). The choline peak (PCh) is increasing with malignancy compared to normal brain, agreeing with [31, 32]. The total Cr concentration decreases with the malignancy as confirmed in [32]. In gliomas, the ratios of NAA/Cr, NAA/Cho, Cr/Cho are significantly decreased compared to those in normal brain (p-value$<$0.05) [33], which we also observe. We notice a relatively constant value for Myo. This is not in contradiction with Tong *et al.* [33], who found a relative elevation of Myo in low-grade astrocytomas when compared with high-grade astrocytomas. The lipid

amplitudes at 0.9 ppm and 1.3 ppm increase with malignancy.

The metabolic images constructed from a patient with a glioblastoma tumour show changes in the concentration of metabolites in the malignant area, which are very plausible. The NAA, Cr, Lac, Lip1 and Lip2 decrease or increase in the malignant area with respect to the healthy area in a similar way as the changes presented in Figure 8 and found in literature. The presence of mobile Lip is thought to correspond to cellular and membrane breakdown corresponding to necrosis [1]. Lactate is usually detected only under pathologic conditions, when energy metabolism is affected severely [31]. The Glu image shows a decrease of Glu in the left ventricle. Similar observations were made in [34]. An increase of PCh, present in the boundary between the malignant and healthy areas could reflect an increase of membrane synthesis and accelerated cell proliferation (see, *e.g.*, [35]). The circled region in Figure 9(g) and (i) corresponds to a region that is slightly higher in intensity in the T2-weighted image. This region has also an increased concentration for Lip2 and Lac. This shows that pathologic information, which is barely visible on MRI images, can be successfully extracted from metabolic maps.

5 Conclusion

In this paper we have shown that AQSES is a robust user friendly short echo time MR quantitation software package. It generates accurate results on simulated data and *in vitro* samples. The results of batches of *in vivo* data that contain spectra from healthy, grade II gliomas and glioblastomas are in line with results described in literature. The results of a set of spectroscopic imaging data is in accordance with MRI images obtained from the same slice. Since the package is open source and written in a flexible language it has the potential to grow rapidly and be of high importance for the medical MR community.

6 Acknowledgements

The Biomedical Magnetic Resonance Research Group Radboud University Nijmegen Medical Center (`http://get.to/mrs`) and the EU funded projects BIOPATTERN (EU network of excellence; Contract No. FP6-2002-IST 508803), INTERPRET (EU shared-cost RTD project; Contract No. FP5-IST-1999-10310), eTUMOUR (FP6-2002-LIFESCIHEALTH; Contract No. 503094) and PDT-COIL (NNE5/2001/887) are gratefully acknowledged.

Research supported by

Research Council KUL: GOA-AMBioRICS, CoE EF/05/006 Optimization in Engineering, several PhD/postdoc & fellow grants;

Flemish Government: FWO: PhD/postdoc grants, projects, G.0407.02 (support vector machines), G.0269.02 (magnetic resonance spectroscopic imaging), G.0270.02 (nonlinear Lp approximation), G.0360.05 (EEG, Epileptic), G.0519.06 (Noninvasive brain oxygenation), research communities (ICCoS, ANMMM); **IWT:** PhD Grants;

Belgian Federal Science Policy Office: IUAP P5/22 ('Dynamical Systems and Control: Computation, Identification and Modelling');

References

[1] S.J. Nelson. Magnetic resonance spectroscopic imaging. *IEEE Engineering in Medicine and Biology Magazine*, pages 30–39, September/October 2004.

[2] F.A. Howe, S.J. Barton, S.A. Cudlip, M. Stubbs, D.E. Saunders, M. Murphy, P. Wilkins, K.S. Opstad, V.L. Doyle, M.C. McLean, B.A. Bell, and J.R. Griffiths. Metabolic profiles of human brain tumours using quantitative in vivo ^{1}H magnetic resonance spectroscopy. *Magnetic Resonance in Medicine*, 49:223–232, 2003.

[3] A.W. Simonetti, W. Melsen, M. van der Graaf, G. Postma, A. Heerschap, and L.M.C. Buydens. A chemometric approach for brain tumor classsification using magnetic resonance imaging and spectroscopy. *Analytical Chemistry*, 75(20):29–36, 2003.

[4] F. Szabo De Edelenyi, C. Rubin, F. Estve, G. Sylvie, M. Dcorps, V. Lefournier, J-F. Le Bas, and C. Rmy. A new approach for analyzing proton magnetic resonance spectroscopic images of brain tumors:nosologic images. *Nature Medicine*, 6:1287–1289, 2000.

[5] B. Wilken, P. Dechent, J. Herms, C. Maxton, E. Markakis, F. Hanefeld, and J. Frahm. Quantitative proton magnetic resonance spectroscopy of focal brain lesions. *Journal of Pediatric Neurology*, 23:22–31, 2000.

[6] M. Castillo, J.K. Smith, and L. Kwock. Correlation of myo-inositol levels and grading of cerebral astrocytomas. *American Journal of Neuroradiology*, 21:1645–1649, 2000.

[7] S.J. Barton, F.A. Howe, A.M. Tomlins, S.A. Cudlip, J.K. Nicholson, B.A. Bell, and J.R. Griffiths. Comparison of in vivo ^{1}H MRS of human brain tumours with ^{1}H HR-MAS spectroscopy of intact biopsy samples in vitro. *Magnetic Resonance Materials in Physics, Biology and Medicine*, 8:121–128, 1999.

[8] M. Rijpkema, J. Schuuring, Y. van der Meulen, M. van der Graaf, H. Bernsen, R. Boerman,

A. van der Kogel, and A. Heerschap. Characterization of oligodendrogliomas using short echo time ^{1}H MR spectroscopic imaging. *NMR in Biomedicine*, 16(1):12–18, 2003.

[9] K.S. Opstad, M.M. Murphy, P.R. Wilkins, B.A. Bell, J.R. Griffiths, and F.A. Howe. Differentiation of metastases from high-grade gliomas using short echo time ^{1}H spectroscopy. *Journal of Magnetic Resonance Imaging*, 20:187–192, 2004.

[10] G. Hagberg, A.P. Burlina, I. Mader, W. Roser, E.W. Radue, and J. Seelig. In vivo proton MR spectroscopy of human gliomas: definition of metabolic coordinates for multidimensional classification. *Magnetic Resonance in Medicine*, 34:242–252, 1995.

[11] D.P. Auer, C. Gossl, T. Schirmer, and M. Czisch. Improved lipid analysis of ^{1}H-MR spectra in the presence of mobile lipids. *Magnetic Resonance in Medicine*, 46:615–618, 2001.

[12] H. Ratiney, M. Sdika, Y. Coenradie, S. Cavassila, D. van Ormondt, and D. Graveron-Demilly. Time-domain semi-parametric estimation based on a metabolite basis set. *NMR in Biomedicine*, 17:1–13, 2004.

[13] S.W. Provencher. Estimation of metabolite concentrations from localized *in vivo* proton NMR spectra. *Magnetic Resonance in Medicine*, 30(6), 1993.

[14] H. Ratiney, Y. Coenradie, S. Cavassila, D. van Ormondt, and D. Graveron-Demilly. Time-domain quantitation of ^{1}H short echo-time signals: Background accommodation. *MAGMA*, 16:284–296, 2004.

[15] J.C. Spall and John P. Garner. Parameter identification of state-space models with nuisance parameters. *IEEE Transactions on Aerospace and Electronic Systems*, 26(6):992–998, 1990.

[16] D.M. Sima and S. Van Huffel. Regularized semiparametric model identification with application to NMR signal quantification with unknown macromolecular baseline. Technical Report 04-229, K.U. Leuven, E.E. Dept. (ESAT-SISTA), Kasteelpark Arenberg 10, 3001 Leuven, Belgium, December 2004. To appear in J. Roy. Stat. Soc. B.

[17] B. De Neuter, L. Vanhamme, P. Lemmerling, and S. Van Huffel. Java-based framework for processing and displaying short-echo-time magnetic resonance spectroscopy signals. Technical report, ESAT-SISTA report, ESAT Laboratory, K.U. Leuven, Belgium, 2004.

[18] U. Klose. In vivo proton spectroscopy in presence of eddy currents. *Magnetic Resonance in Medicine*, 14:26–30, 1990.

[19] T. Laudadio, N. Mastronardi, L. Vanhamme, P. Van Hecke, and S. Van Huffel. Improved lanczos algorithms for blackbox MRS data quantitation. *Journal of Magnetic Resonance*, 157:292–297, 2002.

[20] D.M. Gay. A trust-region approach to linearly constrained optimization. In D. F. Griffiths, editor, *Numerical Analysis Proceedings*, pages 72–105, Dundee, 1983. Springer-Verlag.

[21] T. Sundin, L. Vanhamme, P. Van Hecke, I. Dologlou, and S. Van Huffel. Accurate quantification of ^{1}H spectra: from FIR filter design for solvent suppression to parameter estimation. *Journal of Magnetic Resonance*, 139:189–204, 1999.

[22] C. de Boor. *A Practical Guide to Splines*. Springer, Berlin, 1978.

[23] Paul H.C. Eilers and Brian D. Marx. Flexible smoothing with B-splines and penalties. *Statistical Science*, 11(2):89–121, 1997.

[24] J.J. Moré. The Levenberg-Marquardt algorithm: Implementation and theory. In G.A. Watson, editor, *Numerical Analysis: Proceedings of the Biennial Conference held at Dundee, June 28-July 1, 1977 (Lecture Notes in Mathematics #630)*, pages 104–116. Springer Verlag, 1978.

[25] G.H. Golub and V. Pereyra. The differentiation of pseudo-inverses and nonlinear least squares problems whose variables separate. *SIAM Journal on Numerical Analysis*, 10:413–432, 1973.

[26] G.H. Golub and V. Pereyra. Separable nonlinear least squares: the variable projection method and its applications. *Inverse Problems*, 19(2):1–26, 2003.

[27] U. Seeger and U. Klose. Parameterized evaluation of macromolecules and lipids in proton MR spectroscopy of brain diseases. *Magnetic resonance in Medicine*, 49:19–28, 2003.

[28] International network for pattern of tumours using magnetic resonance. http://carbon.uab.es/INTERPRET/interpret_home.shtml.

[29] D. Sima and S. Van Huffel. Separable nonlinear least squares fitting with linear bound constraints and its application in magnetic resonance spectroscopy data quantification. Technical report, ESAT-SISTA report TR 05-236, ESAT Laboratory, K.U.Leuven, Belgium, 2005.

[30] K.N. Fountas, E.Z. Kapsalaki, S.D. Gotsis, and J.Z. Kapsalakis. In vivo proton magnetic resonance spectroscopy of brain tumors. *Stereotactic and Functional Neurosurgery*, 74:83–94, 2000.

[31] S. Furuya, S. Naruse, M. Ide, H. Morishita, O. Kizu, S. Ueda, and T. Maeda. Evaluation of metabolic heterogeneity in brain tumors using ^{1}H-chemical shift imaging method. *Neurosurgery*, 10:25–30, 1997.

[32] Y. Kinoshita and A. Yokota. Absolute concentrations of metabolites in human brain tumors using in vitro proton magnetic resonance spectroscopy. *NMR in Biomedicine*, 10:2–12, 1997.

[33] Z. Tong, Y. Toshiaki, T. Yamaki, K. Harada, and K. Houkin. In vivo quantification of metabolites in normal brain and brain tumors by proton MR spectroscopy using water as an internal standard. *Magnetic Resonance Imaging*, 22:1017–1024, 2004.

[34] C. Juchem, H. Merkle, N.K. Logothetis, and J. Pfeuffer. In vivo CSI of glutamate in the monkey brain. *Proceedings ISMRM*, page 32, 2004.

[35] G. Fan, B. Sun, Z. Wu, Q. Guo, and Y. Guo. In vivo single-voxel proton MR spectroscopy in the differentiation of high-grade gliomas and solitary metastases. *Clinical Radiology*, 59:77–85, 2004.

Tables

Table 1: Performance measure (PM) for each metabolite of each simulation set (in percentage, see Equation 6). The notations are explained in Section 2.3.

	Myo	PCh	Cr	Glu	NAA	Lac	Lip1	Lip2
exp. 1, Set 1	3.68	1.74	1.31	0.61	0.19	6.09	2.52	0.54
exp. 2, Set 1	13.53	15.16	1.19	0.95	0.94	8.44	2.91	0.54
exp. 3, Set 2	1.39	1.56	0.42	0.8	0.51	12.03	8.58	1.66
exp. 3, Set 3	7.38	5.94	4.14	4.85	3.13	20.22	19.87	7.98
exp. 3, Set 4	11.1	9.83	6.1	8.05	5.78	23.81	34.12	15.52
exp. 3, Set 5	11.67	15.43	4.31	27.92	7.9	29.15	30.55	7.75
exp. 3, Set 6	13.77	16.85	8.01	30.83	11.09	26.42	32.34	18.53

Figure Captions

Figure 1. NAA profile used in the basis set. The amplitudes are in arbitrary units. At 0.0 ppm and 8.44 ppm, the two reference compounds are visible. They are effectively removed by the FIR filter during quantitation.

Figure 2. Simulated spectra from set 4 and set 6. The amplitudes are in arbitrary units.

Figure 3. The AQSES GUI main window.

Figure 4. The AQSES GUI results window.

Figure 5. Boxplot showing the estimated amplitudes of *in vivo* spectra from healthy volunteers.

Figure 6. The left subplot shows the difference between simulated and estimated amplitudes for all profiles in the case no nuisance components are added to the dataset. The right subplot shows the same, but now for data set 6. Clearly, the left figure shows some large errors (mostly from Lac) on a limited number of spectra, while the right figure shows errors on all profiles and all spectra.

Figure 7. *In vitro* test sample results.

Figure 8. Averaged estimated amplitudes for normal tissues, GII and GBM, in arbitrary units.

Figure 9. Metabolic maps of a patient with a glioblastoma.

Figures

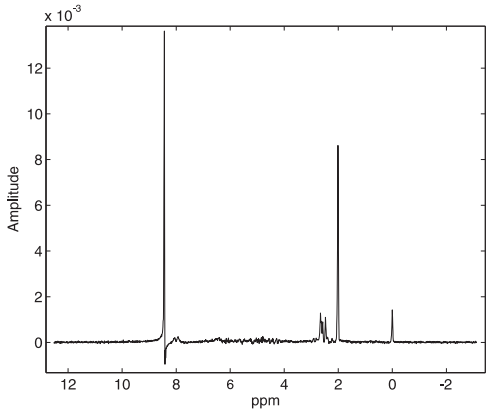
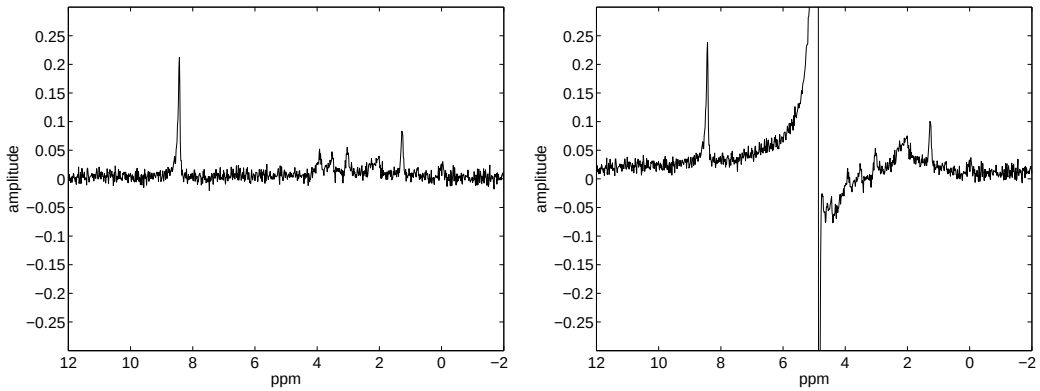


Figure 1: NAA profile used in the basis set. The amplitudes are in arbitrary units. At 0.0 ppm and 8.44 ppm, the two reference compounds are visible. They are effectively removed by the FIR filter during quantitation.



(a) Set 4

(b) Set 6

Figure 2: Simulated spectra from set 4 and set 6. The amplitudes are in arbitrary units.

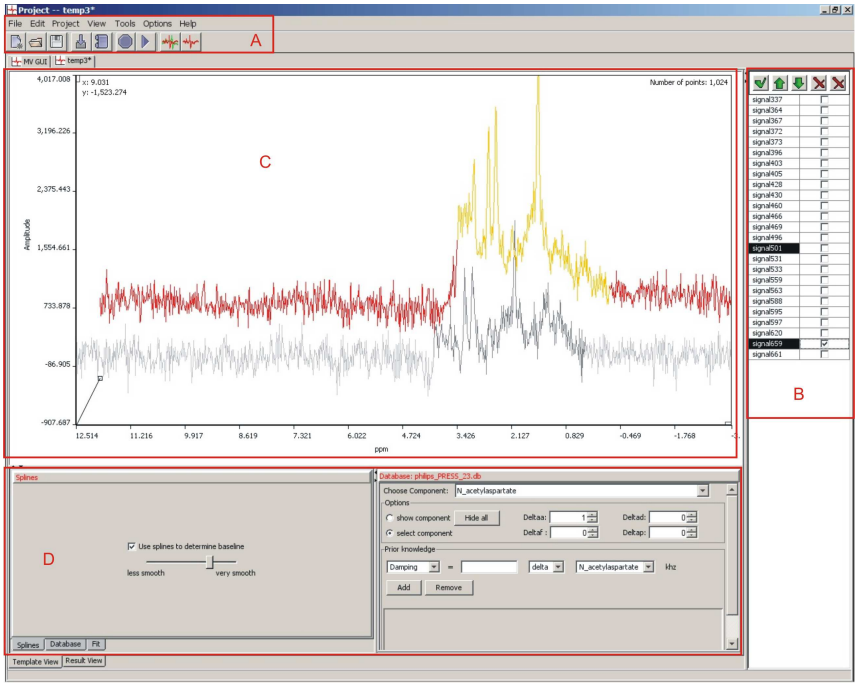


Figure 3: The AQSES GUI main window.

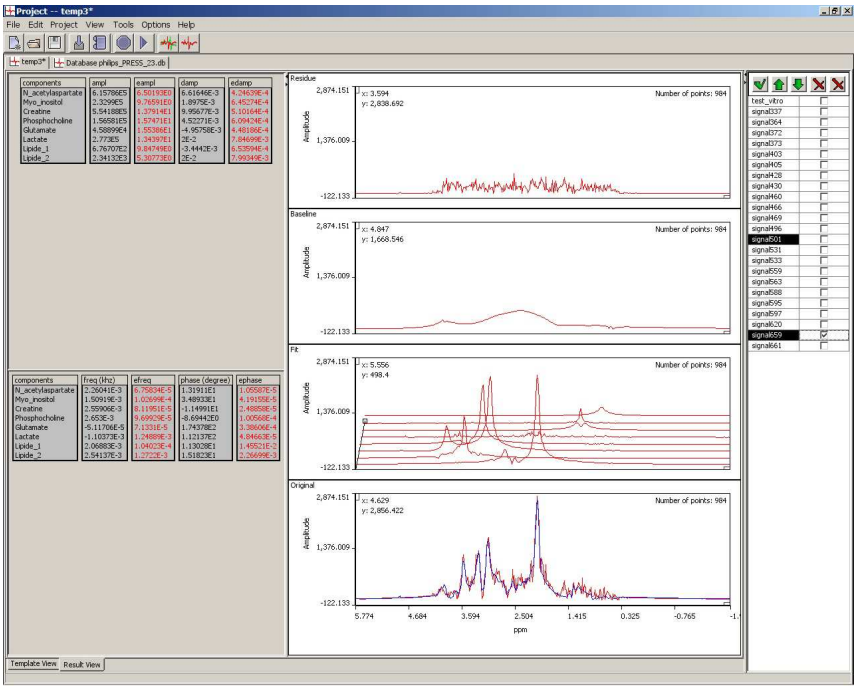


Figure 4: The AQSES GUI results window.

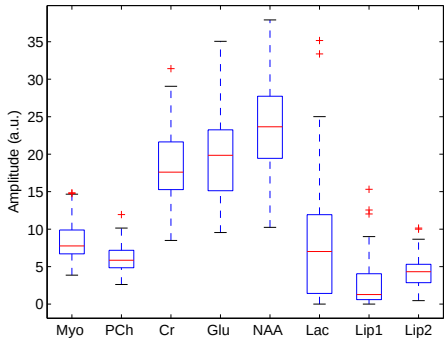


Figure 5: Boxplot showing the estimated amplitudes of *in vivo* spectra from healthy volunteers.

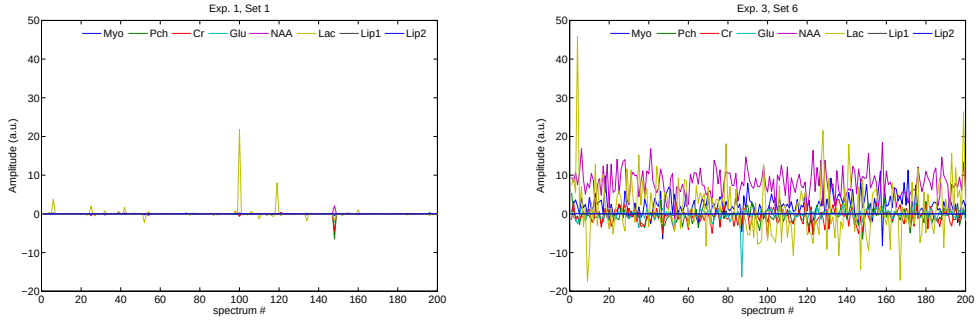


Figure 6: The left subplot shows the difference between simulated and estimated amplitudes for all profiles in the case no nuisance components are added to the dataset. The right subplot shows the same, but now for data set 6. Clearly, the left figure shows some large errors (mostly from Lac) on a limited number of spectra, while the right figure shows errors on all profiles and all spectra.

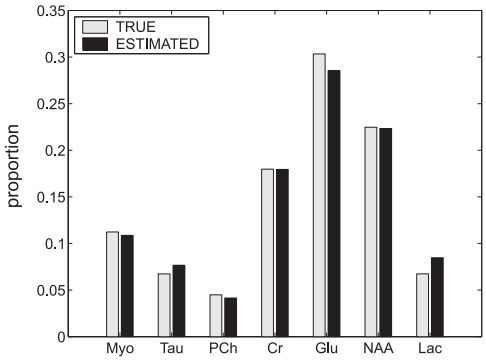


Figure 7: *In vitro* test sample results.

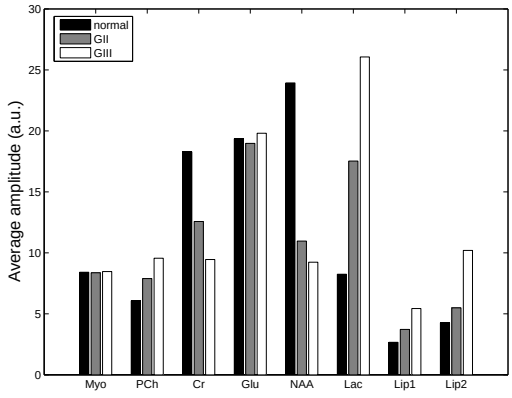


Figure 8: Averaged estimated amplitudes for normal tissues, GII and GBM, in arbitrary units.

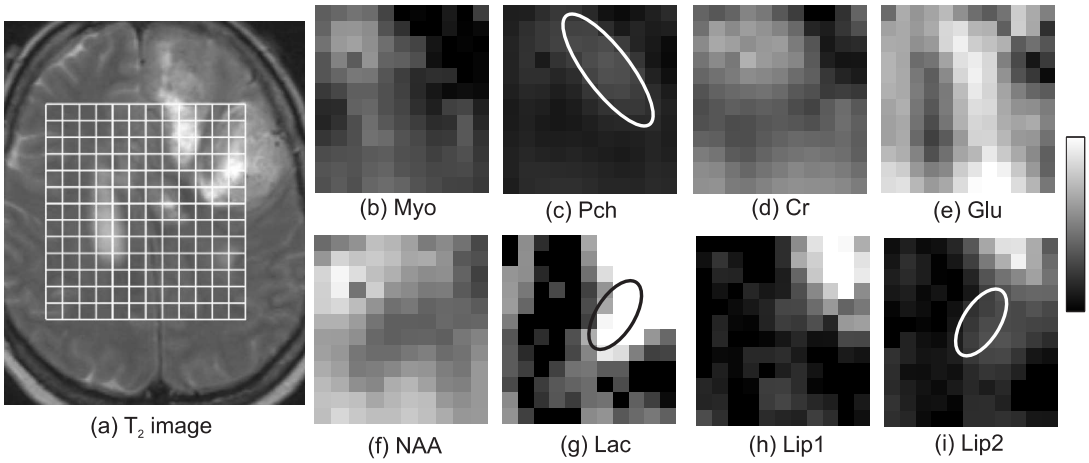


Figure 9: Metabolic maps of a patient with a glioblastoma.